Continental Shelf Research 34 (2012) 79–86

Contents lists available at SciVerse ScienceDirect

Continental Shelf Research

journal homepage: www.elsevier.com/locate/csr

Research papers

Differences in coastal and oceanic SST trends due to the strengthening of coastal upwelling along the Benguela current system

F. Santos [a,*], M. Gomez-Gesteira [a], M. deCastro [a], I. Alvarez [a,b]

[a] EPhysLab (Environmental Physics Laboratory), Universidade de Vigo, Facultade de Ciencias, Ourense, Spain
[b] CESAM, Departamento de Física, Universidade de Aveiro, Aveiro, Portugal

ARTICLE INFO

Article history:
Received 25 May 2011
Received in revised form
29 November 2011
Accepted 7 December 2011
Available online 16 December 2011

Keywords:
Sea surface temperature
Coastal upwelling
Trends
Benguela current ecosystem
Southern annular mode

ABSTRACT

Coastal and oceanic sea surface temperature (SST) trends were analyzed in the Benguela upwelling ecosystem from the seventies on. Monthly SST data were obtained from the UK Meteorological Office, Hadley Center at two transects in front of the Namibia coast and the western coast of South Africa. A positive SST trend (0.06 °C dec^{-1}) is observed at open sea locations and a negative one (−0.13 °C dec^{-1}) near shore. The observed negative ΔSST ($SST_{coast} - SST_{ocean}$) trend (−0.18 °C dec^{-1}) is linked to the strengthening of upwelling (87 m^3 s^{-1} km^{-1} dec^{-1}) during the same period. For this purpose, Ekman transport was directly obtained from the Pacific Fisheries Environmental Laboratory in the area under study and calculated from reanalysis wind data from NCEP/NCAR at six locations in front of the Namibia coast and the western coast of South Africa. This coastal upwelling enhancement is in good agreement with changes in the intensity and location of the South Atlantic High, which are also reflected in the Southern Annular Mode (SAM) index.

1. Introduction

During the last decades numerous studies have tried to quantify trends in sea surface temperature (SST) showing that they are highly dependent on spatial and temporal scales, being possible to observe opposite trends when different temporal periods are considered (Parker et al., 1994; Smith et al., 1994; Casey and Cornillon, 2001). However, most of the studies conclude that a considerable global warming in SST occurred over the last century no matter what data set is considered (Folland et al., 1984, 1992; Parker et al., 1994; Nicholls et al., 1996; Casey and Cornillon, 2001). Global warming is far from being uniform during the 20th century with distinct warming and cooling periods (IPCC, 2007). This global warming is not evenly distributed all over the world's ocean with regions warming faster or slower than the global average (Levitus et al., 2000; Palttridge and Woodruff, 1981). In particular, the Atlantic Ocean contributes most to the increase of the heat content (Nerem et al., 1999; Levitus et al., 2000; Strong et al., 2000). At regional scales, the SST warming rate at coastal and ocean locations placed at the same latitude can be different due to local and remote forcings (Cole et al., 2000; Lemos and Pires, 2004; Ginzburg et al., 2004; Santos et al., 2005; Gómez-Gesteira et al., 2008a; deCastro et al., 2008).

The major upwelling areas all over the world (Canary, California, Peru and Benguela Current System) (Patti et al., 2008) can present important differences in temperature trends compared to surrounding areas due to the intense pumping of deeper water to the surface. In the early 90s Bakun (1990) postulated that under global warming scenario continental air masses warm more rapidly than the oceanic water masses generating a gradient of pressure between the continental low pressure and oceanic high pressure. This greater cross-marging pressure gradient produces a strong equatorward wind stress increasing coastal upwelling along the eastern ocean boundaries. Nevertheless, experimental evidence collected during the last decades has shown contradictory results.

In the Canary current system different results were obtained from previous studies. Bakun (1990) found an intensification of the upwelling favorable winds from 1948 to 1979 and McGregor et al. (2007) obtained a cooling of 0.5 °C during the 20th century associated to an increase of the coastal upwelling. On the contrary, Lemos and Pires (2004) and Lemos and Sansó (2006) found a significant weakening of the upwelling favorable winds during similar periods of time (from 1940 to 2000 and from 1901 to 2000, respectively). Besides, Gómez-Gesteira et al. (2008b) detected a weakening in the upwelling intensity from 1967 to 2006 and Pérez et al. (2010) reported a decrease in the upwelling index, which is even more pronounced during the last four decades (Pardo et al., in press).

In the California current system, Schwing and Mendelssohn (1997) and Mendelssohn and Schwing (2002) found an increase of the coastal upwelling during the favored season linked to

* Corresponding author.
E-mail address: fsantos@uvigo.es (F. Santos).

0278-4343/$ - see front matter © 2011 Elsevier Ltd. All rights reserved.
doi:10.1016/j.csr.2011.12.004

opposite trends in the long-term changes of SST. In addition, Di Lorenzo et al. (2005) also remarked the strengthening of upwelling favorable winds linked to the long term SST warming in this region. Finally, Pardo et al. (in press) did not find a clear trend in the California region during the last six decades.

As far as we know, only a few studies have dealt with the physical component of coastal upwelling trends in Peru and Benguela regions. Pardo et al. (in press) analyzed the Peru region from 1948 to 2009, showing the weakening of upwelling accompanied by a slight SST warming or even cooling trend. The same authors found an enhancement of upwelling with a slight SST warming in the Benguela region. Patti et al. (2010) found a marked increase in wind stress in both regions, with an increase in the water column stability.

The aim of the present study is to characterize the differences in coastal and oceanic SST trends along the Benguela current system and the key role played by the persistent coastal upwelling observed in the region.

2. Benguela current system

The Benguela upwelling ecosystem (BUES) stretches from the southern tip of Africa to about 15°S where it is bounded by the Angola front. The Angola front separates the warm water of the Angola Current from the cold Benguela water. The coastal wind field off Southwest Africa constitutes the main forcing along the BUES (Nelson and Hutchings, 1983; Fennel, 1999). These winds play a key role in coastal dynamics driving upwelling and near shore circulation. The upwelling favorable alongshore wind has a maximum at about 25–27°S and decreases toward the Angola Front and the southern tip of Africa. At this latitude, there is a permanent upwelling region (Shannon, 1985; Shannon and Pillar, 1986), which divides the BUES in two separate sub-ecosystems, the northern and the southern Benguela, whose productivity has been analyzed in previous research (Barange et al., 1991a, b; Fearon et al., 1992; Timonin et al., 1992; Villanueva and Sánchez, 1993; Hewitson and Cruickshank, 1993).

3. Data and processing

SST data were obtained from the UK Meteorological office, Hadley Center HadISST1.1-Global sea-Ice coverage and SST (http://badc.nerc.ac.uk/data/hadisst) (Rayner et al., 2003). Data are available from 1870 on, with monthly periodicity on a $1^\circ \times 1^\circ$ grid with global coverage. In the present study, two transects of 16 data points were considered in front of the Namibia coast and the western coast of South Africa (from 18°S to 35°S): the coastal transect is located near shore and the oceanic transect is located 15° seaward (Fig. 1, empty circles). Only data from 1900 on were considered due to data sparseness during the nineteenth century.

The amplitude of seasonal oscillations in temperature is on the order of 5 °C for the region under study. Using unfiltered data would mask temperature trends, which are on the order of a few tenths of degree in most of the world ocean. Thus, data that were initially retrieved with a monthly periodicity were subsequently averaged at annual scale. This approach removes most of the seasonal variability.

The SST difference between coastal and oceanic transects will be highlighted by means of the SST increment, defined as

$$\Delta SST = SST_{coast} - SST_{ocean} \quad (1)$$

averaged at all coastal and oceanic locations.

Ekman transport data were provided by the Pacific Fisheries Environmental Laboratory (PFEL) (http://www.pfeg.noaa.gov). In the particular area under study, data are available from January 1981 on. For our purposes, monthly Ekman transport data were considered from 15°S to 35°S and from 20°E to 10°W on an approximately $1^\circ \times 1^\circ$ grid.

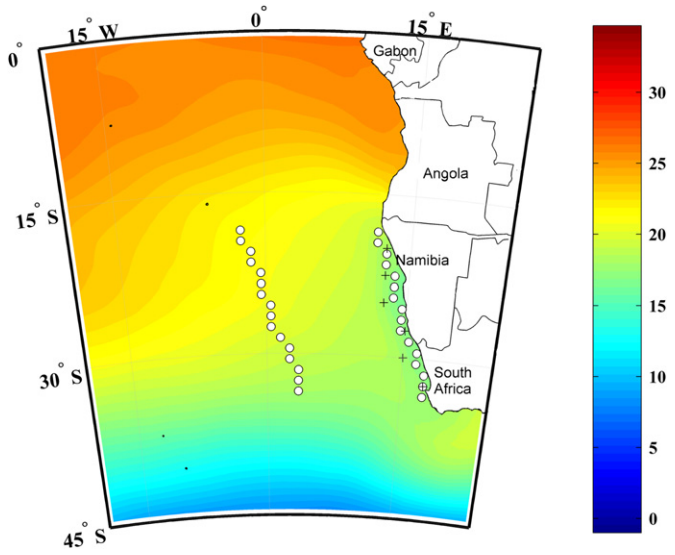

Fig. 1. SST (°C) annual average for the area under study from 1970 to 2009. Black empty circles represent the locations where SST data were extracted. Two transects of 16 points each were considered in front of the Namibia coast and the western coast of South Africa (from 18°S to 35°S). The coastal transect was located at 1 degree from the coast and the oceanic one 15° seaward. White crosses represent a 6-point transect parallel to the shore line where Ekman transport was calculated.

Wind and Sea Level Pressure (SLP) data were also obtained from the National Center of Atmospheric Research/National Center for Environmental Prediction (NCEP/NCAR). Reanalysis Data Archive are available from 1948 onwards, with a global coverage and a spatial resolution of $2.5^\circ \times 2.5^\circ$ (http://www.esrl.noaa.gov/psd/data/reanalysis/reanalysis.shtml). Monthly SLP data from 1970 to 2009 were selected for the present study on a grid covering from 0 to 60°S and from 25°W to 25°E. With respect to wind data, 6 points located in front of the Namibia coast and the western coast of South Africa (from 18°S to 35°S) were considered from 1970 to 2010 (Fig. 1, crosses). These data lie on a spatial grid coarser than the previous ones, although with a longer temporal extent, which allows analyzing trends.

The Ekman transport components can be calculated as follows:

$$Q_x = \frac{\tau_y}{\rho_w f} \text{ and } Q_y = -\frac{\tau_x}{\rho_w f} \quad (2)$$

where

$$\tau_y = \rho_a C_d (W_x^2 + W_y^2)^{1/2} W_y \text{ and } \tau_x = \rho_a C_d (W_x^2 + W_y^2)^{1/2} W_x \quad (3)$$

being τ the wind stress, W the wind speed near surface, ρ_w the sea water density (1025 kg m^{-3}), C_d a dimensionless drag coefficient, (1.4×10^{-3}), ρ_a the air density (1.22 kg m^{-3}) and f is the Coriolis parameter defined as twice the vertical component of the Earth's angular velocity, Ω, about the local vertical given by $f = 2\Omega \sin(\theta)$ at latitude θ. Finally, x subscript corresponds to the zonal component and the y subscript to the meridional one.

Upwelling Index (UI) can be defined as the Ekman transport component in the direction perpendicular to the shoreline (Nykjaer and Van Camp, 1994). UI was calculated at the 6-point transect mentioned above (Fig. 1, crosses) following (Gómez-Gesteira

et al., 2006):

$$UI = -(\sin(\theta-\pi/2)Q_x + \cos(\theta-\pi/2)Q_y) \quad (2)$$

where θ is the mean angle between the shore line and the Equator. $\theta = 112.5^\circ$ was considered to be the mean coastal angle in this study. Using this definition, positive (negative) upwelling indices correspond to upwelling-favorable (unfavorable) conditions.

The principal mode of atmospheric variability in the Southern Hemisphere extratropics and high latitudes is the Southern Hemisphere Annular Mode (SAM). The SAM index is defined as the difference in the normalized monthly zonal mean of SLP between 40°S and 70°S (Nan and Li, 2003). This index is a modification of the Antarctic Oscillation (AAO) index defined as the difference in the normalized monthly zonal mean of SLP between 40°S and 65°S (Gong and Wang, 1999). The SAM index shows a stronger negative correlation in the zonal mean SLP anomalies than that between 40°S and 65°S (Nan and Li, 2003).

4. Results and discussion

The annual SST average in the area under study from 1970 to 2009 (Fig. 1) highlights the interruption of the normal north–south SST gradient in the area by the intrusion of cooler water (around 16 °C) near the Namibia coast. This representation shows the Benguela upwelling system stretching from the southern tip of Africa to about 15°S, where it is bounded by the Angola front.

The inter-annual evolution of SST meridionally averaged from 18°S to 35°S was depicted for the period 1900–2009 (Fig. 2(a)). This analysis was carried out at different distances from the coast, from 1° (bottom line) till 15° (top line). A running average of ±5 years was used to smooth out high frequency variations in temperature. In general, an average increment in SST was obtained for the unfiltered signal at all distances from the coast for the period 1900–2009 (0.07–0.08 °C dec^{-1}, $P<0.01$). This warming is similar to that described by Rayner et al. (2006) for the Southern Hemisphere, who found a temperature change of 0.68 ± 0.18 °C from 1901 to 2004 using a linear trend. Other authors, Folland et al. (1990), found an increase of 0.38–0.58° C for the Southern Hemisphere from 1861 to 1989.

Nevertheless, cooling can be observed at transects near the coast (lower lines) during the last decades, whilst warming is still present at ocean all location (upper lines). Two procedures were considered in order to determine the breakpoint between periods with significantly different trends. The first one, following the method described by Tome and Miranda (2004), shows a break point in 1972 for transects placed at 1 and 2° from the coast. The second method, which was also applied to the same transects, is based on the absolute maximum calculation of the filtered SST signal for the whole period. In this case, the maximum appears in 1968. The mean between the values obtained from both procedures, 1970, was considered in this study.

SST trends were calculated from 1970 to 2009 (Fig. 2(b)). X axis represents the distance (in degrees) from transect to shore. Dots represent SST trends, small circles correspond to trends with $0.01<P<0.1$ and large circles correspond to trends with $P<0.01$. Near coast transects show significant negative trends. The most negative trend is obtained for the near-shore transect (−0.13 °C dec^{-1}, $P<0.01$). The trend decreases for transect located at two degrees from the coast (−0.06 °C dec^{-1}, $P<0.1$). No significant trends are observed for transects located at 3 and 4° from the coast. Significant positive trends are observed for rest of transects, where a nearly constant value is shown (0.05 − 0.06 °C dec^{-1}, $P<0.1$). Note that the cooling observed near coast during the last decades is lower than the warming suffered from 1900 to 1970. Actually, the warming observed for that period was about 0.16 °C dec^{-1}. Overall, the coastal region has warmed from 1900 to 2009 at a rate of −0.13 °C dec^{-1}.

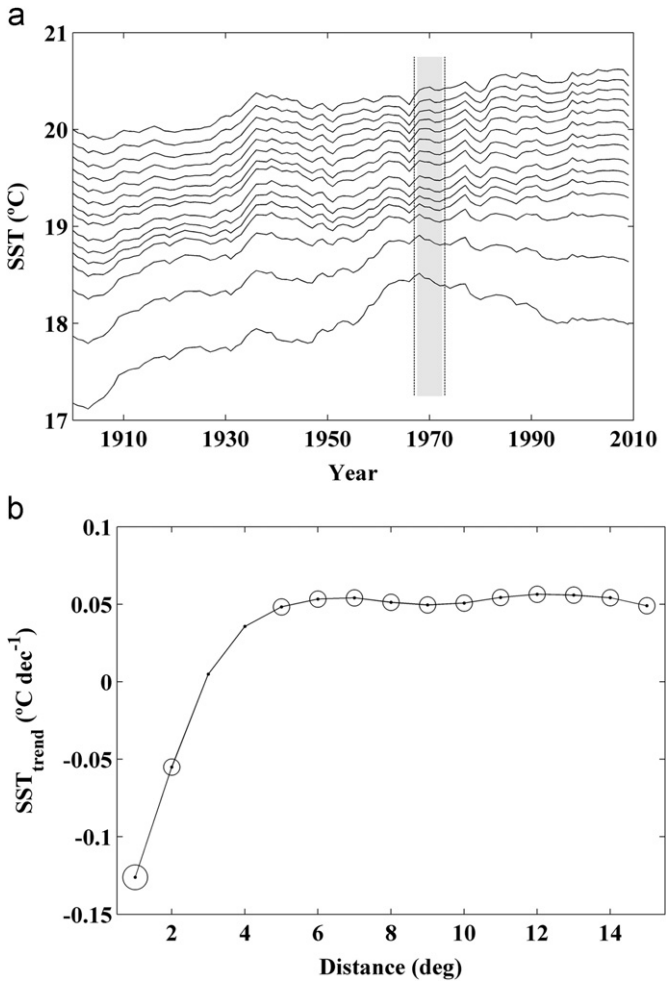

Fig. 2. (a) Inter-annual variation of SST (°C) meridionally averaged from 18°S to 35°S at different distances from the coast for the period 1900–2009. Bottom line represents transect located at 1° from the coast and the top line represents transect located 15° from the coast. A running average of ±5 years was used to smooth high frequency variations in temperature. The shadow area between vertical lines marks the break point between periods with significantly different coastal SST trends (1970). (b) SST trends calculated from 1970 to 2009. X axis represents the transect distance (in degrees) from the coast. Dots represent SST trends, small circles correspond to trends with $0.01<P<0.1$ and large circles correspond to trends with $P<0.01$.

The increase of oceanic SST from the seventies on had been reported in previous studies at global and regional scale (IPCC, 2007; Garcia-Soto et al., 2002; deCastro et al., 2009; Gómez-Gesteira et al. 2011; Pardo et al., in press). The ocean trend observed in BUES (0.06 °C dec^{-1}) is not far from the one calculated by Casey and Cornillon (2001) for the Southeast Atlantic using the COADS dataset and a temperature class binning scheme and the period 1960 − 1990 (0.09 ± 0.07 °C dec^{-1}). The BUES ocean warming is lower than observed in the North Atlantic (0.2–0.3 °C dec^{-1}) for the last three decades (deCastro et al., 2009; Goikoetxea et al., 2009; Michel et al., 2009; Gómez-Gesteira et al., 2011). As for coastal SST, the observed cooling has not been detected in previous studies carried out in the same area (Pardo et al., in press), probably due to the coarseness of the SST grid used by those authors. The observed cooling in BUES (−0.13 °C dec^{-1}) contrasts with the warming reported in other coastal areas (e.g. Gómez-Gesteira et al. (2008a) calculated a mean warming of 0.23 °C dec^{-1} in the North Atlantic Arc).

Macroscopically, the annual SST tendency from 1970 to 2009 is also shown in Fig. 3. Negative values, ranging from 0 to $-0.25\ ^{\circ}C\ dec^{-1}$, are observed near to the coast and positive values, ranging from 0 to $0.15\ ^{\circ}C\ dec^{-1}$, at the open ocean. The patterns detected at annual scale can also be reproduced at seasonal scale (Fig. 4a–d). Thus, the near shore area tends to cool and the ocean area to warm at all seasons. The coastal cooling is more intense during January–March (JFM) and April–June (AMJ) and the ocean warming is more intense during October–December (OND).

Fig. 5 shows the different warming rate at coastal and oceanic locations. Note that ΔSST is always negative since coastal water is cooler than oceanic water due to the presence of persistent upwelling (Nelson and Hutchings, 1983; Fennel, 1999). A running average of ± 5 years was applied to smooth the signal only for representation purposes. A significant negative trend ($-0.18\ ^{\circ}C\ dec^{-1}$, $P<0.01$) was observed for the unfiltered signal. This trend is consistent with the warming (cooling) at ocean (coastal) areas described above.

The negative trend detected in the ΔSST from 1970 to 2009 is possibly related to the strengthening of persistent coastal upwelling in the Benguela region. To characterize this coastal upwelling system, the Ekman transport field averaged from 1981 to 2009 was analyzed in Fig. 6(a) using data from the PFEL. Annual Ekman transport field shows the strongest values (between 1500 and 2000 $m^3\ s^{-1}\ km^{-1}$) near the Namibia coast perpendicular to the shoreline and pointing seaward. In addition, the annual cycle of UI was calculated at the 6 points marked with crosses in Fig. 1 using NCEP/NCAR data from 1970 to 2009 (Fig. 6(b)). The annual cycle is always positive (upwelling favorable conditions) showing its persistent character throughout the year. The maximum UI values were obtained at 25°S during the austral spring and summer (values close to 2000 $m^3\ s^{-1}\ km^{-1}$). Since the general behavior of UI is similar at all latitudes (positive and more intense during spring and summer), the UI annual cycle was meridionally averaged from 20°S to 32°S (Fig. 6(c)). The UI amplitude ranges from around 400 $m^3\ s^{-1}\ km^{-1}$ during MJJ to around 1300 $m^3\ s^{-1}\ km^{-1}$ during NDJ. Error bars were calculated using the standard deviation of the monthly data, σ(UI), divided by the square root of the number of data.

The UI trend was calculated from 1970 to 2009 (Fig. 7). UI was spatially averaged for the 6 points along the BUES (white crosses in Fig. 1). A running average of ± 5 year was applied to smooth the signal for representation. A clear positive trend can be observed for the unfiltered signal ($87\ m^3 s^{-1}\ km^{-1}\ dec^{-1}$, $P<0.01$). A similar general enhancement of the upwelling intensity in the BUES was detected by Pardo et al. (in press) with values raging from 20 ± 3 to $100\pm4\ m^3\ s^{-1}\ km^{-1}\ dec^{-1}$ for the last four decades. Trends in the rest of the mayor upwelling systems all over the world have been

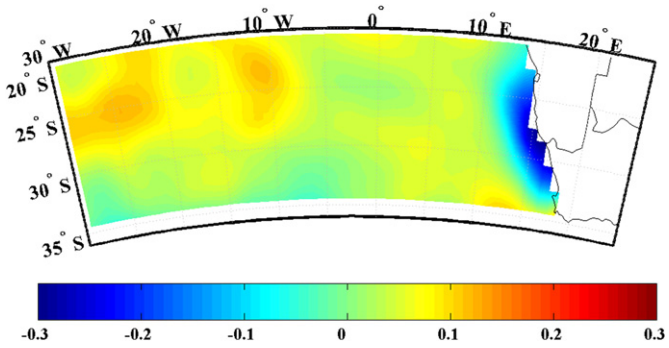

Fig. 3. Annual SST trend ($^{\circ}C\ dec^{-1}$) for the area under study from 1970 to 2009.

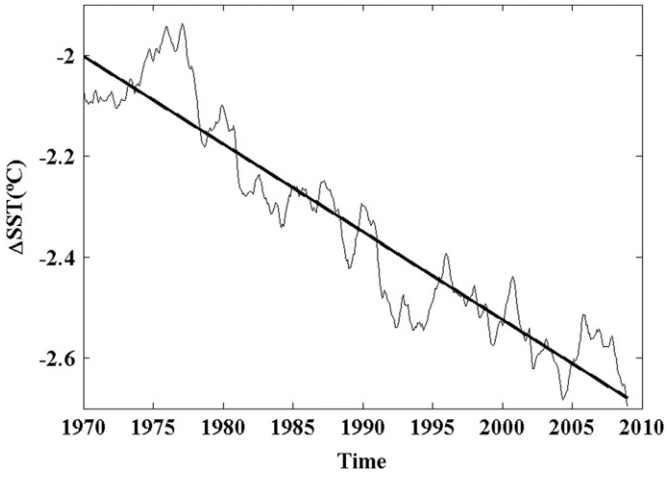

Fig. 5. Inter-annual variation of $\Delta SST = SST_{coast} - SST_{ocean}$ (°C) from 1970 to 2009. A running average of ± 5 years was used to smooth high frequency variations in temperature. The solid line represents a linear trend of $-0.18\ ^{\circ}C\ dec^{-1}$ ($P<0.01$).

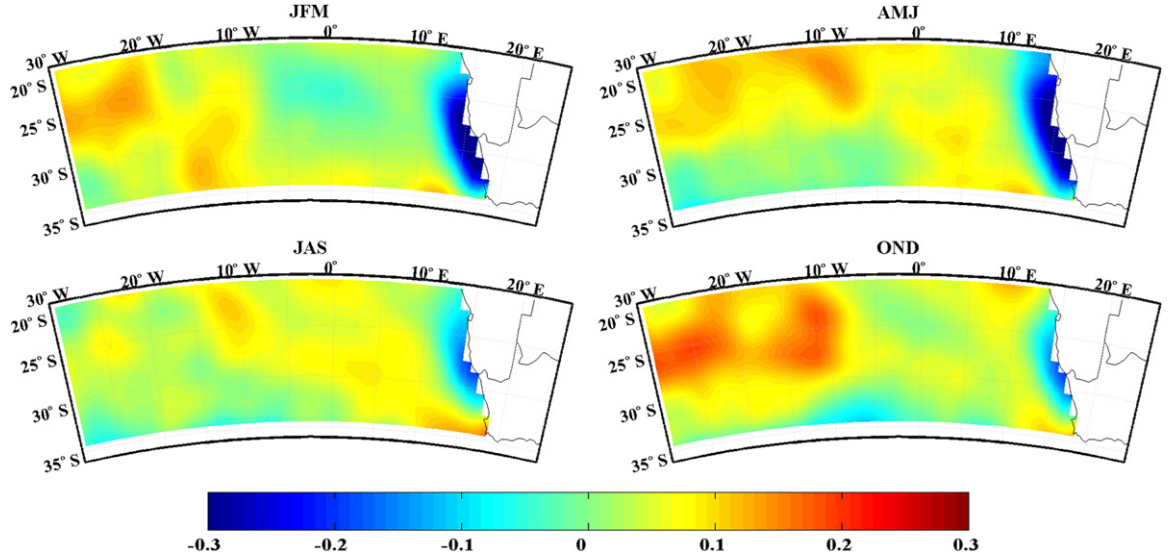

Fig. 4. Seasonal SST trend ($^{\circ}C\ dec^{-1}$) for the area under study from 1970 to 2009. (a) January–March (JFM); (b) April–June (AMJ); (c) July–September (JAS) and (d) October–December (OND).

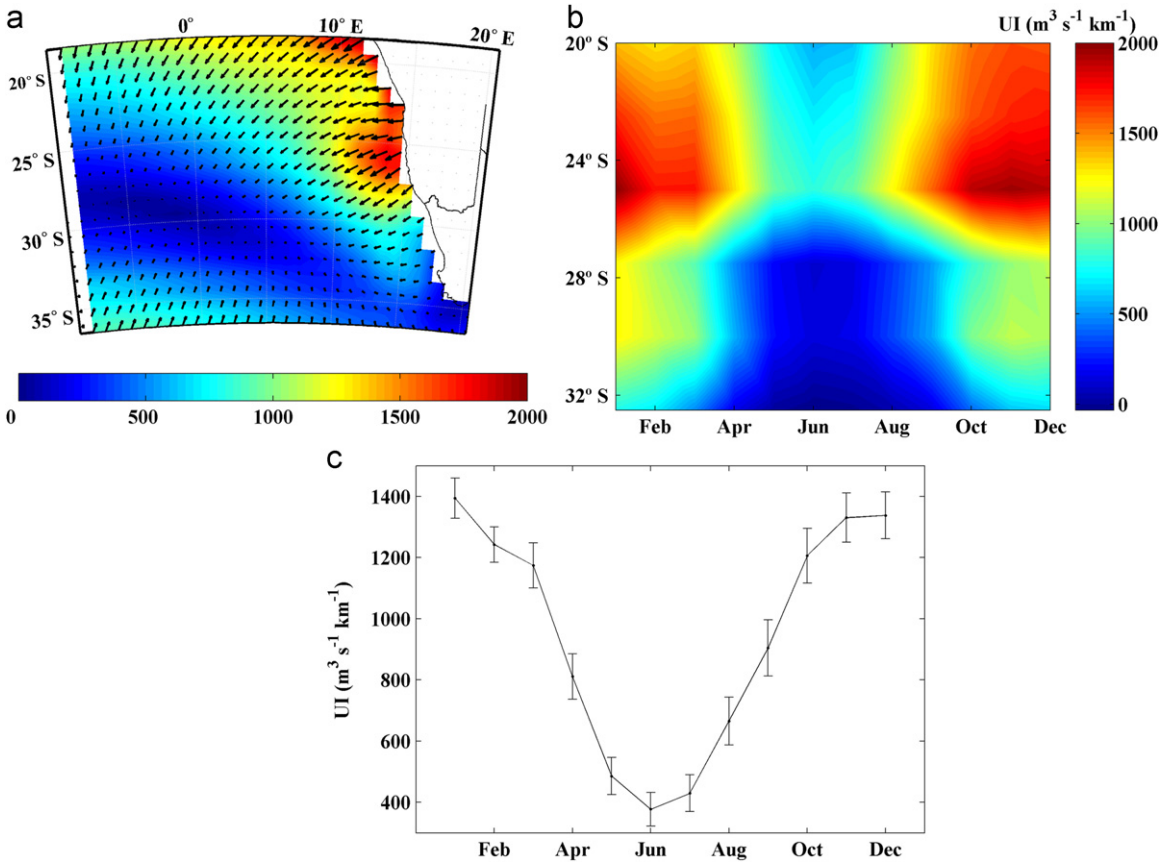

Fig. 6. (a) Ekman transport field ($m^3\,s^{-1}\,km^{-1}$) averaged using PFEL data for the area under scope from 1981 to 2009; (b) annual cycle of UI ($m^3\,s^{-1}\,km^{-1}$) for the six points along the BUES (crosses in Fig. 1) calculated using NCEP/NCAR data for the period 1970 to 2009; (c) annual UI cycle ($m^3\,s^{-1}\,km^{-1}$) meridionally averaged from 20°S to 32°S for the period 1970 to 2009. Error bars were calculated using the standard deviation of the monthly data, σ(UI), divided by the square root of the number of data.

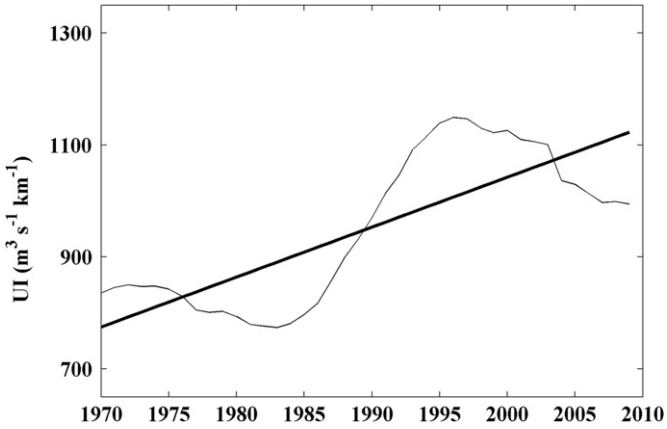

Fig. 7. UI variability from 1970 to 2009. UI was spatially averaged for the 6 points parallel to the BUES (crosses in Fig. 1). A running average of ± 5 year was used to smooth high frequency variations in UI. The straight line represents the linear trend with a slope of 87 $m^3\,s^{-1}\,km^{-1}\,dec^{-1}$($P<0.01$).

Table 1
Monthly upwelling trends corresponding to the period 1970–2009.

Month	*UI* ($m^3\,s^{-1}\,km^{-1}\,yr^{-1}$)
Jan	16.5*
Feb	16.4*
Mar	12.5*
Apr	5.7*
May	3.1*
Jun	4.3*
Jul	2.5**
Aug	3.4**
Sep	5.4*
Oct	11.8*
Nov	10.7*
Dec	14.4*

* $P<0.01$.
** $P<0.05$.

considered by other authors (Schwing and Mendelssohn, 1997; Mendelssohn and Schwing, 2002; Lemos and Pires, 2004; Di Lorenzo et al., 2005; Lemos and Sansó, 2006; Gómez-Gesteira et al., 2008b; Patti et al., 2010; Pardo et al., in press).

Trends in Benguela UI were also characterized at monthly scale from 1970 to 2009 (Table 1). All months show a significant positive trend, ranging from 25 $m^3\,s^{-1}\,km^{-1}\,dec^{-1}$ in July to 165 $m^3\,s^{-1}\,km^{-1}\,dec^{-1}$ in January. In general, the higher the upwelling intensity (ONDJFM in Fig. 6(c)) the greater the trend.

The obtained UI trends can be explained in terms of a general atmospheric circulation pattern. In fact, several authors have reported the significant influence of the SAM index in the Southern Hemisphere climate variability (Kidson, 1999; Baldwing, 2001; Nan and Li., 2003) and in the large-scale variability of the Southern Ocean (Hall and Visbeck, 2002). In addition, several authors (see Marshall, 2003 and the references therein) have observed a trend in the SAM index toward its positive phase and analyzed its influence on zonal winds. The inter-annual variability of the monthly SAM index from 1970 to 2009 shows a clear positive trend with a slope of 0.37 dec^{-1} and $P<0.01$ (Fig. 8). This

trend represents an increase in the positive phase of the SAM index of approximately 20% during the period 1970–2009.

The positive phase of the SAM index represents relatively low pressures over Antarctica compared to those of mid latitudes. Thus, the evolution of the South Atlantic High can be analyzed for the period under study. The annual SLP averaged from 1970 to 2009 (Fig. 9(a)) shows a SLP maximum (SLP^{max}) of 102,246 Pa located at mid latitudes (30.63°S and 5.45°W). SLP anomalies were used to characterize the inter-annual evolution of the SLP^{max} from 1970 to 2009 (Fig. 9(b)). A clear positive trend of 14 Pa dec^{-1} ($P=0.06$) is observed, reflecting the strengthening of the South Atlantic High from the seventies onward. In addition, the displacement of the High during the last four decades was also analyzed. A clear negative trend ($-0.18°$ dec^{-1}, $P=0.07$) is observed in latitude anomaly (Fig. 9(c)) and a positive one ($0.27°$ dec^{-1} without statistical significance) in longitude anomaly (Fig. 9(d)). This fact represents a southeastward drift of the South Atlantic High, approaching the BUES coast, which can also result in the strengthening of coastal winds.

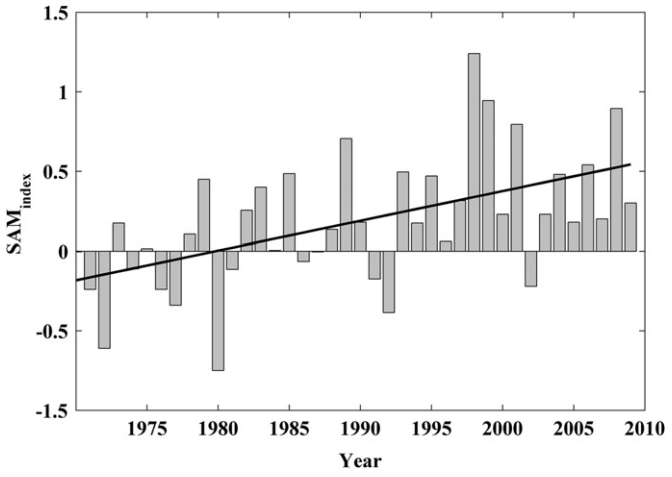

Fig. 8. Monthly Southern Annular Mode (SAM) index from 1970 to 2009 (gray bars). The solid black line represents a linear trend of 0.37 dec^{-1} ($P<0.01$).

5. Concluding remarks

The warming observed from the seventies onward at global scales might not be present or might even change sing in coastal areas due to the existence of some local forcing. Thus, in the Benguela upwelling ecosystem, the moderate ocean warming observed at the adjacent area (0.06 °C dec^{-1}) was reversed by the strengthening in coastal upwelling, which resulted in water cooling near shore (-0.13 °C dec^{-1}). This enhancement in coastal upwelling (87 m^3 s^{-1} km^{-1} dec^{-1}) is in good agreement with the trend toward the positive phase (0.37 dec^{-1}) observed in the SAM index. Upwelling strengthening is also consistent with changes in the intensity and position of the South Atlantic High. The intensity was observed to increase in about 14 Pa dec^{-1}, and the position was observed to drift southeastward ($-0.18°$ dec^{-1}

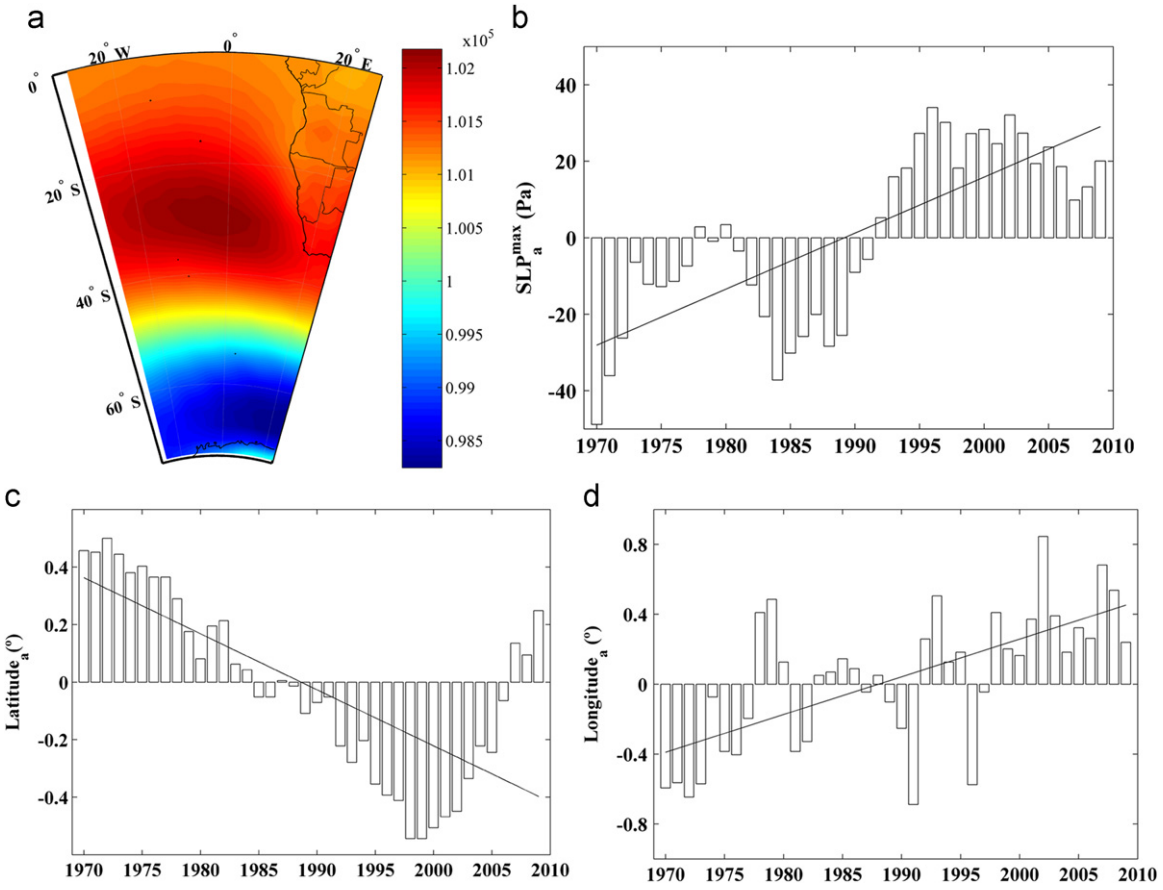

Fig. 9. Evolution of the South Atlantic High from 1970 to 2009. (a) Mean SLP (in 10^5 Pa). The SLP maximum (SLP^{max}) is located at mid latitudes (30.6°S, 5.4°W) with a value of 102,246 Pa. (b) Evolution of SLP^{max} anomaly (bars). The dark line represents the linear tendency (14 Pa dec^{-1}, $P=0.06$). (c) Displacement in the latitude of the SLP^{max} relative to the mean position (bars). The dark line represents the trend ($-0.19°$ dec^{-1}, $P=0.07$). (d) Displacement in the longitude of the SLP^{max} relative to the mean position (bars). The dark line represents the trend ($0.27°$ dec^{-1} without statistical significance).

in latitude and 0.27° dec^{-1} in longitude) approaching the coast and enhancing coastal winds.

Acknowledgments

This work is partially supported by the Sunta de Galicia under project 10PXIB 383169PR. I. Alvarez is supported by the Ministerio de Ciencia e Innovación through the Ramón y Cajal Program. This work was partially supported by Xunta de Galicia under Programa de Consolidación e Estruturación de Unidades de Investigación (Grupos de Referencia Competitiva) funded by European Regional Development Fund (FEDER).

References

Bakun, A., 1990. Global climate change and intensification of coastal upwelling. Science 247, 198–201. doi:10.1126/science.247.4939.198.

Baldwin, M.P., 2001. Annular modes in global daily surface pressure. Geophysical Research Letters 28, 4115–4118.

Barange, M., Gibbons, M.J., Carola, M., 1991a. Diet and feeding of Euphausiahanseni and Nematoscelismegalops (Euphausiacea) in the northern Benguela current: ecological significance of vertical space partitioning. Marine Ecology Progress Series 73, 173–181.

Barange, M., Guitierrez, E., Flos, J., 1991b. Variability of particulate organic carbon and nitrogen in the Namibian upwelling system. Marine Biology 110 (3), 409–418.

Casey, K.S., Cornillon, P., 2001. Global and regional sea-surface temperature trends. Journal of Climate 14, 3801–3818.

Cole, J.E., Dunbar, R.B., McClanahan, T.R., Muthiga, N.A, 2000. Tropical Pacific forcing of decadal SST variability in the western Indian Ocean over the past two centuries. Science 287, 617–619.

deCastro, M., Gomez-Gesteira, M., Lorenzo, M.N., Alvarez, I., Crespo, A.J.C., 2008. Influence of atmospheric modes on coastal upwelling along the western coast of the Iberian Peninsula, 1985–2005. Climate Research 36, 169–179.

deCastro, M., Gomez-Gesteira, M., Alvarez, I., Gesteira, J.L.G., 2009. Present warming within the context of cooling–warming cycles observed since 1854 in the Bay of Biscay. Continental Shelf Research 29, 1053–1059.

Di Lorenzo, E., Miller, A.J., Schneider, N., McWilliams, J.C., 2005. The warming of the California current system: dynamics and ecosystem implications. Journal of Physical Oceanography 35, 336–362. doi:10.1175/JPO-2690.1.

Fearon, J.J., Boyd, A.J., Schuülein, F.H., 1992. Views on the biomass and distribution of Chrysaorahysoscella (Linne, 1766) and Aequoreaaequorea (Forskal, 1775) off Namibia, 1982–1989. Scientia Marina 56 (1), 75–85.

Fennel, W., 1999. Theory of the Benguela upwelling system. Journal of Physical Oceanography 29, 177–190.

Folland, C., Parker, D., Kates, F., 1984. Worldwide marine temperature fluctuations 1856–1981. Nature 310, 670–673.

Folland, C., Karl, T., Vinnikov, K., 1990. Observed climate variations and change. In: Houghton, J., Jenkins, G., Ephraums, J. (Eds.), Climate Change: The IPCC Scientific Assessment. , Cambridge University Press, pp. 195–238.

Folland, C., Nicholls, N., Nyenzi, B., Parker, B., Vinnikov, K., 1992. Observed climate variability and change. In: Houghton, J., Jenkins, G., Ephraums, J. (Eds.), Climate Change 1992: The Supplementary Report to the IPCC Scientific Assessment. Cambridge University Press, pp. 135–170.

Garcia-Soto, C., Pingree, R.D., Valdés, L., 2002. Navidad development in the Southern Bay of Biscay: climate change and Swoddy structure from remote sensing and in situ measurements. Journal of Geophysical Research 107. doi:10.1029/2001JC001012 (C8 3118).

Ginzburg, A.I., Kostianoy, A.G., Sheremet, N.A., 2004. Seasonal and interanual variability of the Black Sea surface temperature as revealed from satellite data (1982–2000). Journal of Marine Systems 52, 33–50.

Goikoetxea, N., Borja, A., Fontán, A., González, M., Valencia, V., 2009. Trends andanomalies in sea surface temperature, observed over the last 60 years, within the southeastern Bay of Biscay. Continental Shelf Research 29, 1060–1069. doi:10.1016/j.csr.2008.11.014.

Gómez-Gesteira, M., Moreira, C., Alvarez, I., deCastro, M., 2006. Ekman transport along the Galician coast (NW, Spain) calculated from forecasted winds. Journal of Geophysical Research. 111, C10005. doi:10.1029/2005JC003331.0.

Gómez-Gesteira, M., deCastro, M., Álvarez, I., Gómez-Gesteira, J.L., 2008a. Coastal sea surface temperature warming trend along the continental part of Atlantic Arc (1985–2005). Journal of Geophysical Research 113, C04010. doi:10.1029/2007JC004315.

Gómez-Gesteira, M., deCastro, M., Álvarez, I., Lorenzo, M.N., Gesteira, J.L.G., Crespo, A.J.C, 2008b. Spatio-temporal upwelling trends along the Canary upwelling system (1967–2006). In: Trends and Directions in climate Research. Annals New York Academy Science vol. 1146, pp. 320–337.

Gómez-Gesteira, M., Gimeno, L., deCastro, M., Lorenzo, M.N., Alvarez, I., Nieto, R., Taboada, J.J., Crespo, A.J.C., Ramos, A.M., Iglesias, I., Gómez-Gesteira, J.L., Santo, F.E., Barriopedro, D., Trigo, I.F., 2011. The state of climate in north–west Iberia. Climate Research. doi:10.3354/cr00967.

Gong, D.Y., Wang, S.W., 1999. Definition of Antarctic oscillation index. Geophysical Research Letters 26, 459–462.

Hall, A., Visbeck, M., 2002. Synchronous variability in the Southern Hemisphere atmosphere, sea ice, and ocean resulting from the annular mode. Journal of Climate 15, 3043–3057.

Hewitson, J.D., Cruickshank, R.A., 1993. Production and consumption by planktivorous fish in the Northern Benguela ecosystem in the 1980s. South African Journal of Marine Science 13, 15–24.

Intergovernmental Panel on Climate Change, 2007. Climate Change 2007: the physical science basis. Contribution of Working Group 1 to the Fourth Assessment Report of the Intergovernmental panel on Climate Change. Cambridge University Press, Cambridge, UK.

Kidson, J.W., 1999. Principal modes of Southern Hemisphere lowfrequency variability obtained from NCEP–NCAR reanalysis. Journal of Climate 12, 2808–2830.

Lemos, R.T., Pires, H.O., 2004. The upwelling regime off the west Portuguese coast, 1941–2000. International Journal of Climatology 24, 511–524. doi:10.1002/joc.1009.

Lemos, R.T., Sansó, H.O., 2006. Spatio-temporal variability of ocean temperature in the Portugal current system. Journal of Geophysical Research 111, C04010. doi:10.1029/2005JC003051.

Levitus, S., Antonov, J.I., Timothy, P.B., Stephens, C., 2000. Warming of the world ocean. Science 287, 2225–2229.

Michel, S., Treguier, A.M., Vandermeirsch, F., 2009. Temperature variability in the Bay of Biscay during the past 40 years, from an in situ analysis and a 3D global simulation. Continental Shelf Research 29 (8), 1070–1087. doi:10.1016/j.csr.2008.11.019.

Marshall, G.J., 2003. Trends in the southern annular mode from observations and reanalysis. Journal of Climate 16, 4134–4143.

McGregor, H.V., Dima, M., Fischer, H.W., Mulitza, S., 2007. Rapid 20th-century increase in coastal upwelling off northwest Africa. Science 315, 637–663. doi:10.1126/science.1134839.

Mendelssohn, R., Schwing, F.B., 2002. Common and uncommon trends in SST and wind stress in the California and Peru–Chile current systems. Progress in Oceanography 53, 141–162.

Nan, S., Li, J., 2003. The relationship between the summer precipitation in the Yangtze River valley and the boreal spring Southern Hemisphere annular mode. Geophysical Research Letters 30 (24), 2266. doi:10.1029/2003GL018381.

Nelson, G., Hutchings, L., 1983. The Benguela upwelling area. Progress in Oceanography 12, 333–356.

Nerem, R.S., Chambers, D.P., Leuliette, E.W., Mitchum, G.T., Giese, B.S., 1999. Variations in global mean sea level associated with the 1997–1998 ENSO event: implications for measuring long-term sea level change. Geophysical Research Letters 26, 3005–3008.

Nicholls, N., Gruza, G.V., Jouzel, J., Karl, T., Ogallo, L., Parker, D., 1996. Observed climate variability and change. In: Houghton, J., Jenkins, G., Ephraums, J. (Eds.), Climate Change 1995: The Science of Climate Change. , Cambridge University Press, pp. 133–192.

Nykjaer, L., Van Camp, L., 1994. Seasonal and interannual variability of coastal upwelling along northwest Africa and Portugal from 1981 to 1991. Journal of Geophysical Research 99 (C7), 14197–14207.

Palttridge, G., Woodruff, S., 1981. Changes in global surface temperature from 1880 to 1977 derived from historical records of sea surface temperature. Monthly Weather Review 109, 2427–2434.

Pardo, P.C., Padín, X.A., Gilcoto, M, Fariña-Busto, L., Pérez, F.F. Evolution of upwelling systems coupled to the long term variability of sea surface temperature and Ekman transport. Climate Research. doi:10.3354/cr00989, in press (reference number C 989).

Parker, D.E., Jones, P., Folland, C., Bevan, A., 1994. Interdecadal changes of surface temperature since the late nineteenth century. Journal of Geophysical Research 99, 14339–14373.

Patti, B., Guisande, C., Vergara, A.R., Riveiro, I., Maneiro, I., Barreiro, A., Bonanno, A., Buscaino, G., Cuttitta, A., Basilone, G., Mazzola, S., 2008. Factors responsible for the differences in satellite-based chlorophyll a concentration between the major global upwelling areas. Estuarine, Coastal and Shelf Science 76, 775–786. doi:10.1016/j.ecss.2007.08.005.

Patti, B., Guisande, C., Riveiro, I., Thejil, P., Cuttitta, A., Bonanno, A., Basilone, G., Buscaino, G., Mazzola, S., 2010. Effect of atmospheric CO_2 and solar activity on wind regime and water column stability in the major global upwelling areas. Estuarine Coastal and Shelf Science 88, 45–52.

Pérez, F.F., Padín, X.A., Pazos, Y., Gilcoto, M., Cabanas, M., Pardo, P.C., Doval, M.D., Fariña-Busto, L., 2010. Plankton response to weakening of the Iberian coastal upwelling. Global Change Biology 16, 1258–1267. doi:10.1111/j.1365-2486.2009.02125.x.

Rayner, N.A., Parker, D.E., Horton, E.B., Folland, C.K., Alexander, L.V., Rowell, D.P., Kent, E.C., Kaplan, A., 2003. Global analyses of sea surface temperature, sea ice, and night marine air temperature since the late nineteenth century. Journal of Geophysical Research 108 (D14), 4407.

Rayner, N.A., et al., 2006. Improved analyses of changes and uncertainties in sea surface temperature measured in situ since the mid-nineteenth century: the HadSST2 data set. Journal of Climate 19, 446–469.

Santos, A.M.P., Kazmin, A.S., Peliz, A., 2005. Decadal changes in the Canary upwelling system as revealed by satellite observations: their impact on productivity. Journal of Marine Research 63, 359–379.

Schwing, F.B., Mendelssohn, R., 1997. Increased coastal upwelling in the California current system. Journal of Geophysical Research 102, 3421–3438.

Shannon, L.V., 1985. The Benguela ecosystem. Part 1. Evolution of the Benguela, physical features and processes. Oceanography and Marine Biology: An Annual Review 23, 105–182.

Shannon, L.V., Pillar, S.C., 1986. The Benguela ecosystem. Part III. Plankton. Oceanography and Marine Biology: An Annual Review 24, 65–170.

Smith, T.M., Reynolds, R.W., Ropelewski, C.F., 1994. Optimal averaging of seasonal sea-surface temperatures and associated confidence intervals (1860–1989). Journal of Climate 7, 949–964.

Strong, A.E., Kearns, E.J., Gjovig, K.K., 2000. Sea surface temperature signals from satellite—an update. Geophysical Research Letters 27, 1667–1670.

Tome, A.R., Miranda, P.M.A., 2004. Piecewise linear fitting and trend changing points of climate parameters. Geophysical Research Letters 31, L02207. doi:10.1029/2003GL019100.

Timonin, A.G., Araschkevich, E.G., Drits, A.V., Semenova, T.N., 1992. Zooplankton dynamics in the northern Benguela ecosystem, with special reference to the copepod Calanoidescarinatus. South African Journal of Marine Science 12, 545–560.

Villanueva, R., Sánchez, P., 1993. Cephalopods of the Benguela current off Namibia: new additions and considerations on the genus *Lycoteuthis*. Journal of Natural History 27 (1), 15–46.